JOURNAL OF AGRICULTURAL AND FOOD CHEMISTRY
ARTICLE

J. Agric. Food Chem. 2009, 57, 5201–5210 5201
DOI:10.1021/jf803818y

In Vitro and *in Vivo* Anti-angiogenic Activities and Inhibition of Hormone-Dependent and -Independent Breast Cancer Cells by Ceramide Methylaminoethylphosphonate

Madhavi Chintalapati,[†] Robert Truax,[‡] Rhett Stout,[§] Ralph Portier,[∥] and Jack N. Losso*,[†]

[†]Department of Food Science and [‡]Biotechnology Laboratory, Louisiana State University Agriculture Center and [§]School of Veterinary Medicine and [∥]Department of Environmental Sciences, Louisiana State University, Baton Rouge, Louisiana 70803

Ceramide methylaminoethylphosphonate (CMAEPn) was isolated from eastern oyster (*Crassostrea virginica*) and screened against *in vitro* and *in vivo* angiogenesis and against MCF-7 and MDA-MB-435s breast cancer cell lines. *In vitro* angiogenesis was evaluated by the vascular endothelial growth factor (VEGF)-induced human umbilical vein endothelial cell (HUVEC) tube formation assay. MCF-7 and MDA-MB-435s cell viability was evaluated by the CellTiter 96 AQ_{ueous} One Solution Cell Proliferation assay. Apoptosis was evaluated by the caspase-9 assay, autophagy by acridine orange staining and beclin-1 level. Our study indicates that CMAEPn at 50 μM inhibited VEGF-induced tube formation by HUVEC. The viability of MCF-7 and MDA-MB-435s breast cancer cells exposed to 125 μM CMAEPn for 48 h was reduced to 76 and 85%, respectively. The viability of MCF-7 and MDA-MB-435s cells exposed to 250 μM CMAEPn for 48 h under the same conditions was reduced to 38 and 45%, respectively. CMAEPn at 125 μM inhibited VEGF-induced MDA-MB-435s cell migration and invasion. CMAEPn at 125 μM also decreased VEGF, EGF levels in the conditioned media, PI3K, IκB phosphorylation and degradation in the cytoplasmic extracts, and NFκB nuclear translocation. Both acridine orange staining and beclin-1 indicated autophagic cell death in MCF-7 and MDA-MB-435s cells, respectively. *In vivo*, CMAEPn at 30 mg/kg body weight inhibited bFGF-induced angiogenesis and caused a 57% reduction in hemoglobin levels in the matrigel plug assay within 7 days. This is the first report on CMAEPn-inhibited angiogenesis both *in vitro* and *in vivo*.

KEYWORDS: Ceramide methylaminoethylphosphonate; angiogenesis; breast cancer cells; matrigel plug assay; autophagy; VEGF; PI3K; beclin-1; IκB; NFκB

1. INTRODUCTION

Ceramide methylaminoethylphosphonate (CMAEPn) and ceramide aminoethylphosphonate (CAEPn) are naturally occurring sphingophosphonolipids (**Figure 1**) widely distributed in marine invertebrates, including several freshwater and marine bivalves, snails, edible mollusks, jellyfish, shellfish, gastropods of land as well as freshwater and marine origin, and anemones (*1*−*6*). CMAEPn and CAEPn consist of 2-aminoethylphosphonic acid substituted on the primary hydroxyl group of a characteristic sphingosine base (*7*). The structure of CMAEPn, which consists of a C−P bond, is highly resistant to endogenous hydrolytic enzymes, and the presence of CMAEPn as a cell membrane structural molecule and its highly ionic nature may play a role in membrane permeability to small ions from an aqueous environment into the intercellular space of the invertebrate and stabilization against the effects of hydrolytic enzymes, such as phospholipases and phosphatases, which are very active in the gastrointestinal tract of these marine species (*7*). Phosphonolipids may play a role in the inhibition of phosphatidylinositol-3-kinase, which is known to stimulate cell division and inhibit apoptosis in several cell types; however, data to confirm or refute this hypothesis have never been reported (*8*). The occurrence of 2-aminoethylphosphonic acid in human tissues has been reported possibly as a result of ingestion of shellfish (*7*).

Many anticancer drugs presently used in clinical practice are natural products (such as vinca alkaloids and taxoids) or derivatives of natural products (such as ectoposides). In this respect, marine invertebrates provide a significant resource or lead for the discovery of novel, small molecules for biomedical and pharmaceutical applications. The structure of CMAEPn in marine invertebrates was reported for the first time in sea anemone (*9*). The presence of CAEPn in oyster (*Ostrea gigas*) was reported for the first time by Matsubara and Hayashi (*10*). In oyster, CMAEPn is concentrated in adductor, gills, mantle, and viscera (*2*). The identification in oyster of bioactive compounds that can inhibit phosphatidylinositol-3-kinase presents a health interest because oysters are food sources commercially available

*To whom correspondence should be addressed. Telephone: (225) 578-3883. Fax: (225) 578-5300. E-mail: jlosso@lsu.edu.

 Published on Web 05/28/2009

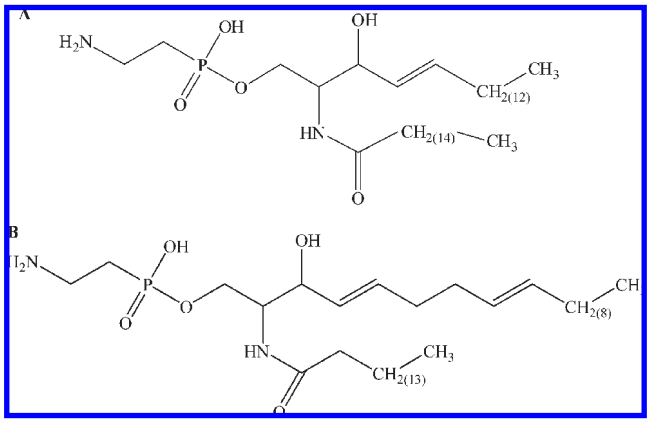

Figure 1. Structures of (A) CMAEPn and (B) CAEPn.

throughout the Gulf of Mexico, having a high degree of consumption and export. Several studies have suggested that treating cancer cells *in vitro* and *in vivo* with exogenous ceramides, such as C_2-ceramide, almost always causes cancer cell death by inhibition of cell growth and induction of apoptosis (*11*−*15*). However, on the other hand, several studies have indicated that the metabolites of ceramides, including sphingosine 1-phosphate (S1P) and glucosphingolipids, play opposing roles and induce transformation, cancer cell growth and proliferation, or angiogenesis (*11*, *15*). Exogenous ceramides that are nontoxic, resistant to endogenous hydrolytic enzymes, bioavailable, and can be incorporated into lipid matrix while retaining activity against biomarkers of cell proliferation may be an asset for targeting tumor cells *in vivo*. Here, we describe the isolation, activity, and mechanism of action of CMAEPn derived from eastern oysters (*Crassostrea virginica*) that potently induce cell death in hormone-dependent and -independent breast cancer and angiogenic endothelial cells *in vitro* and *in vivo*. The findings were confirmed *in vitro* using the angiogenesis assay and breast cancer cell viability and *in vivo* using the matrigel plug assay.

2. MATERIALS AND METHODS

2.1. Materials. Oyster samples were obtained from P and J in New Orleans, LA, and Motivatit in Houma, LA. CellTiter 96 AQ_{ueous} One Solution Cell Proliferation assay and Caspase-9 assay kits were obtained from Promega (Madison, WI). The *in vitro* angiogenesis kit ECM 625 was purchased from Chemicon (Temecula, CA). Cell migration and cell invasion kits were purchased from Cell Biolabs (San Diego, CA). TransAM Nuclear Extract and TransAM-NFκB kits were purchased from Active Motif (Carlsbad, CA). *DC* Protein assay kit was purchased from Bio-Rad (Richmond, CA). Human vascular endothelial growth factor (VEGF) and EGF enzyme-linked immunosorbent assay (ELISA) kits were purchased from Peprotech (Rock Hill, NJ). Anti-PI3K antibodies were obtained from Lab Vision (Fremont, CA). Rabbit anti-beclin-1 polyclonal antibody was obtained from Novus Biologicals (Littleton, CO). Acridine orange, 3-methyladenine (3-MA), and anti-β actin were purchased from Sigma (St. Louis, MO). Gels for electrophoresis, transfer membranes, and Western Blot kits were from Invitrogen (Carlsbad, CA). All other reagents were of analytical grade.

2.2. Cell Lines and Culture Conditions. Human umbilical vein endothelial cells (HUVECs) were obtained from Clonetics, a division of Lonza (Walkerswvlle, MD). Cells were grown at 37 °C in a 5% CO_2 atmosphere in a humidified incubator. The medium used was EGM-2 Bulletkit (Cambrex-Lonza). Procedures used for maintaining and culturing cells were supplied by Lonza. Normal human breast cells Hs578 Bst, estrogen-dependent MCF-7, and estrogen-independent MDA-MB-435s cell lines were obtained from American Type Culture Collection (ATCC) (Manassas, VA) and cultured in Dulbecco's modified Eagle medium (DMEM) high glucose (Invitrogen, Carlsbad, CA) supplemented with sodium bicarbonate (3.7 g/L), 15 mM *N*-2-hydroxyethylpiperazine-*N*′-2-ethanesulfonic acid (HEPES), 10% fetal bovine serum (FBS) (Hyclone, Logan, UT), Glutamax (Invitrogen, Carlsbad, CA), non-essential amino acids (Sigma, St. Louis, MO), and sodium pyruvate (Sigma, St. Louis, MO). Insulin−transferrin−selenium (ITS) was added to the media of MCF-7 cells. Cells were grown at 37 °C in a 5% CO_2 atmosphere in a humidified incubator.

2.3. Isolation and Purification of CMAEPn. CMAEPn was purified using a modification of the method of Matsubara et al. (*1*) and de Souza et al. (*5*) and identified by electrospray ionization−mass spectrometry (ESI−MS) in the positive mode using a PE Sciex Qstar (Quadrupole-TOF hybrid, Applied Biosystems, Foster City, CA). The spectrum was recorded at an accelerating voltage of 4500 V. A purified sample of CAEPn (*16*) was also obtained from Dr. Saki Itonori, Shiga University, Japan.

2.4. *In Vitro* Anti-angiogenic Activity of CMAEPn. HUVEC tube formation on matrigel (ECM matrix) was conducted as suggested by the manufacturer. Briefly, 50 μL of ECM matrix (matrigel) solution at 4 °C was added to 96-well plates and allowed to solidify and polymerize at 37 °C and 5% CO_2 for 1 h. HUVECs were suspended at the concentration of 1.0×10^4 cells per 100 μL in culture medium (RPMI) containing 10 ng/mL VEGF and 0−100 μM CMAEPn dissolved in dimethylsulfoxide (DMSO), with the final DMSO concentration being less than 0.1%. Cells were carefully layered on top of the polymerized gel, and the plates were incubated for 6 h at 37 °C and 5% CO_2 in a humidified incubator. Tube formation was inspected and photographed using a Leitz phase-contrast inverted microscope at 40× magnification.

2.5. Cell Viability and Proliferation Assay. Normal human breast cells Hs578 Bst and MCF-7 and MDA-MB-435s breast cancer cells at 2×10^4 cells/well were seeded in 96-well plates in a total volume of 0.1 mL in serum-containing medium and allowed to adhere overnight. The following morning, the MCF-7 cells were treated with 10 ng/mL 17β-estradiol. The MCF-7 and MDA-MB-435s cells were treated with 0−500 μM CMAEPn dissolved in DMSO, making sure that the DMSO concentration did not exceed 0.1%. All experiments were carried out in triplicates. Replicates of culture plates were prepared and incubated for 24, 48, or 72 h in a humidified incubator containing 5% CO_2 at 37 °C. Cell viability was determined by the CellTiter 96 AQ_{ueous} One Solution Cell Proliferation assay as follows. A total of 20 μL of the reagent was added to control and treated cells; the plate was incubated for 1 h at 37 °C; and the absorbance was read at 490 nm using a Spectra Max *Plus* (Molecular Devices, Sunnyvale, CA). Cell viability and proliferation were normalized to the levels in untreated control cells to determine the percentage of viable cells.

2.6. VEGF and EGF Quantification by ELISA. VEGF and EGF proteins released in the conditioned media were measured using commercial ELISA kits for VEGF or EGF (Preprotech, Rock Hill, NJ) following the instructions of the manufacturer. MCF-7 or MDA-MB-435s cells (5×10^4/well) were seeded in 12-well plates for 24 h, rinsed with phosphate-buffered saline (PBS) twice, and incubated with 0−250 μM CMAEPn (for MCF-7) and 0−500 μM CMAEPn (for MDA-MB-435s) at 37 °C and 5% CO_2 for 48 h. Negative controls were incubated with the medium. The supernatants were collected for analysis. Assays were performed in triplicate, repeated at least 3 times, and expressed in pg/mL as mean ± standard error of the mean (SEM).

2.7. Cell Migration Assay. The assay was carried using a CytoSelect 96-well Cell Invasion Assay (Cell Biolabs, Inc., San Diego, CA) following the instructions of the manufacturer. MDA-MB-435s cells suspended at 1.0×10^6 cells/0.1 mL in serum-free media and treated with or without CMAEPn (0−125 μM CMAEPn) were seeded in the upper chamber. The wells of the feeder tray (lower chamber) were loaded with 150 μL of media containing 10 ng/mL VEGF. After incubation for 6 h at 37 °C in a 5% CO_2 atmosphere, the cells that migrated through 8 μm pore size to the lower chamber were dislodged from the underside of the membrane and lysed in the presence of CyQuant GR dye solution, 150 μL of the mixture was transferred to a 96-well plate suitable for fluorescence measurement, and the plate was read at 480/520 nm using a Perkin-Elmer LS 50B spectrofluorometer. Each assay was conducted in triplicate and repeated at least 3 times.

2.8. Quantification of Apoptosis. The Caspase-Glo 9 assay kit (Promega, Madison, WI) was used according to the instructions of the manufacturer. Briefly, MCF-7 and MDA-MB-435s cells in 96-well plates were treated with 0, 125, or 250 μM CMAEPn, respectively, and incubated for 48 h. At the end of the incubation period, the cells

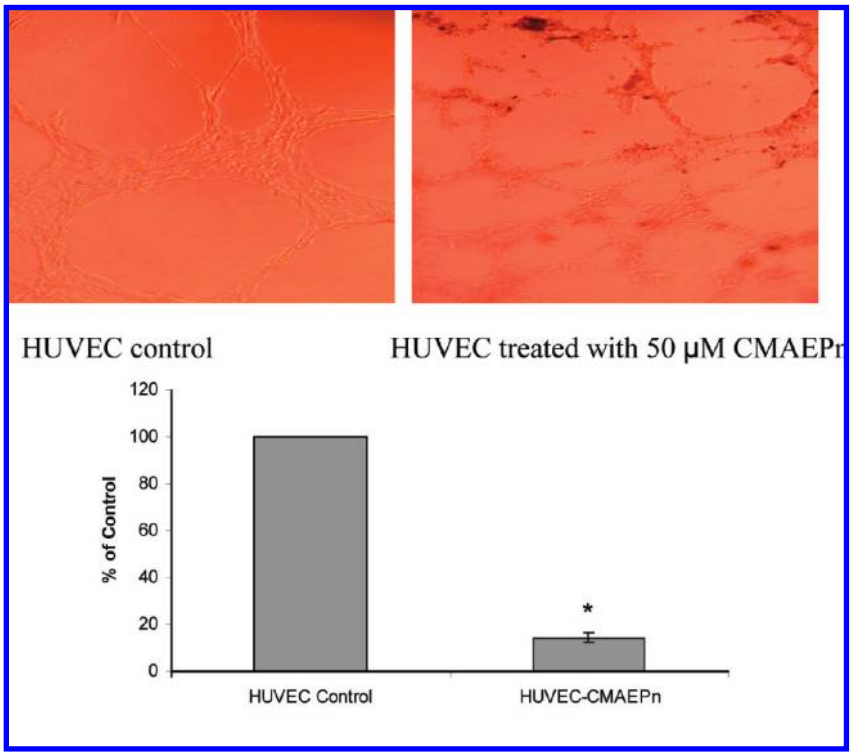

Figure 2. Inhibitory effect of CMAEPn on tube formation induced by VEGF. HUVECs were seeded in matrigel-coated plates containing 10 ng/mL VEGF and indicated the concentration of CMAEPn for 6 h at 37 °C in 5% CO_2, and then they were observed and photographed under a microscope (magnification of 40×).

were treated with 100 μL of Caspase-Glo 9 reagent incubated for 1 h and the luminescence of the solution was measured using a Perkin-Elmer LS 50B luminometer.

2.9. Induction of Autophagic Vacuoles by CMAEPn. For visualization of autophagic vacuoles, MCF-7 and MDA-MB-435s cells in 6-well plates were treated with or without CMAEPn for 48 h and incubated with medium containing 1 μg/mL acridine orange (Molecular Probes, Eugene, OR) for 15 min (*17*). After removal of acridine orange, fluorescent micrographs were taken using an inverted fluorescent microscope (*18*).

2.10. Protein Extraction and Western Blot. MCF-7 and MDA-MB-435s cells grown to confluence were serum-starved for 24 h and treated with or without a wide range of CMAEPn concentrations for 48 h. The cells were washed with ice-cold PBS (pH 7.4) and lysed with ice-cold RIPA buffer [50 mM Tris-HCl, 150 mM NaCl, 1% Nonidet P-40, 0.5% sodium deoxycholate, and 0.1% sodium dodecyl sulfate (SDS)] containing 2 mM phenylmethylsulphonyl fluoride (PMSF), 1 mM sodium orthovanadate, 20 μg/mL aprotinin, 2 μg/mL leupeptin, and 1 μg/mL pepstatin for 30 min at 4 °C. Total cell lysates were centrifuged at 15000*g* for 10 min, and the supernatants were recovered in separate eppendorf test tubes. Protein concentrations in lysate supernatants were determined using *DC* Protein assay (Bio-Rad). For immunoprecipitation, 300 μg of cell extract was incubated with anti-PI3K or anti-beclin-1 at 4 °C on an end-to-end rotator. The supernatant was centrifuged at 10000*g* for 10 min, and protein A/G beads were added. The mixture was rotated for 3 h at 4 °C, and the immunocomplexes were washed with lysis buffer 3 times. LDS sample buffer was added to the beads, and the beads were incubated at 95 °C for 5 min. The supernatant was subjected to Western Blot analysis. Proteins were separated by electrophoresis using 4−12% Bis-Tris gels (Invitrogen) and transferred to nitrocellulose membrane. Membranes were blocked with 5% nonfat dry milk in PBS/Tween 20 (0.05%), followed by incubation with an anti-PI3K antibody (1:1000 in 10% milk/PBS-T), anti-beclin-1 (1:1000), or anti-β actin (for equal loading). Visualization of the bound primary antibody was performed by probing with alkaline phosphatase-conjugated secondary antibody and exposure to a Western breeze chromogenic detection reagent (Invitrogen).

2.11. Quantification of IκBα Degradation and Nuclear Factor κB (NFκB) DNA-Binding Activity. MCF-7 and MDA-MB-435s cells were stimulated with 10 ng/mL TNF-α and simultaneously treated with increasing concentrations of CMAEPn. The degradation of IκBα in cytoplasmic extracts of control and CMAEPn-treated cells was determined by ELISA using a kit from Active Motif (Carlsbad, CA). NFκB p50/65 DNA-binding activity in the nuclear extracts of control and CMAEPn-treated MCF-7 and MDA-MB-435s cells was determined by ELISA using a kit from Active Motif (Carlsbad, CA).

2.12. *In Vivo* Anti-angiogenic Activity of CMAEPn. We used the matrigel sponge model of angiogenesis (BD Biosciences, Franklin Lakes, NJ). A total of 6-week old female Sprague−Dawley rats were purchased from an in-house breeding colony and housed in the Vivarium of the School of Veterinary Medicine at Louisiana State University. All of the animal protocols were performed in accordance with the guidelines and regulations approved by the Louisiana State University Institutional Animal Care and Use Committee. Animals were anesthetized with isoflurane (2−3%) via nose cone and 100% oxygen used as the carrier gas; the flank was shaved and disinfected with ethyl alcohol. A total of 1 mL of matrigel mixed with 300 ng of bFGF was injected subcutaneously without CMAEPn on the left flank and with 30 mg/kg body weight of CMAEPn on the right flank. After 7 days, the matrigel plugs were carefully removed from underneath the skin, photographed, and analyzed for hemoglobin concentration using Drabkins reagent. The absorbance was read at 540 nm in an ELISA plate reader (Spectra Max Plus, Molecular Devices, Sunnyvale, CA). The experiment was repeated twice with five animals, and hemoglobin values are expressed as milligrams of hemoglobin per milliliter of plug.

2.13. Statistical Analysis. All experiments were repeated at least twice. Data are presented as mean ± standard error (SE). The treatment effects were analyzed by paired *t* test, one-way analysis of variance (ANOVA). Differences were considered to be statistically significant when $p < 0.05$. In the case of Western Blot data, one representative set of results is shown.

3. RESULTS

3.1. Inhibition of *in Vitro* Angiogenesis. In the presence of 10 ng/mL VEGF, HUVEC plated on the EC matrix aligned and formed capillary-like structures within 6 h (**Figure 2**).

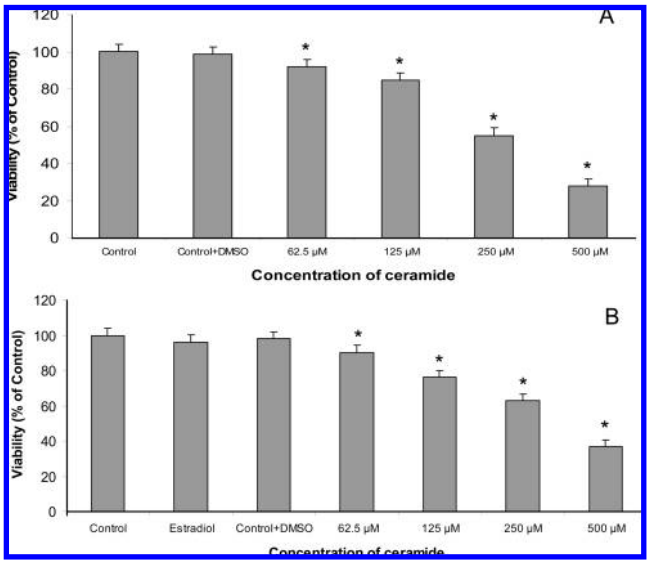

Figure 3. Effect of CMAEPn on VEGF-induced MCF-7 and MDA-MB-435s cell viability. The inhibitory effect of CMAEPn on VEGF-induced cell viability was measured by the CellTiter 96 AQ_{ueous} One Solution Cell Proliferation assay as described in section . The effect of CMAEPn on MCF-7 cell viability is shown in A, and the effect of CMAEPn on MDA-MB-435s cell viability is shown in B. Results are expressed as a percentage of the control (DMSO treated) and are means ± SEM of three replicates from at least three experiments. (*) $p < 0.05$ versus control.

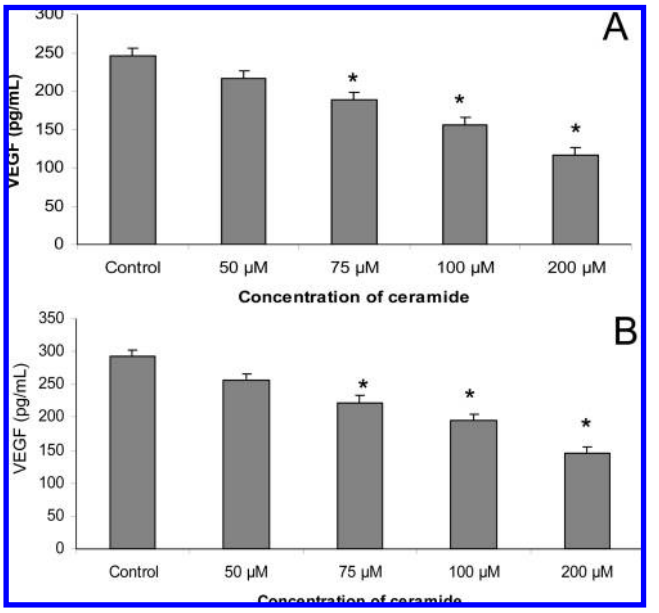

Figure 4. Effect of CMAEPn on secreted VEGF in cell cultures. Cells were serum-starved overnight and exposed to 0−200 μM CMAEPn (for MCF-7, A) or 0−500 μM CMAEPn (for MDA-MB-435s, B) for 48 h before harvesting the conditioned medium. VEGF protein secreted in the medium was detected by the ELISA assay. Data represent the mean values ± SEM of three replicates from at least three experiments. (*) $p < 0.05$ compared to the control cells.

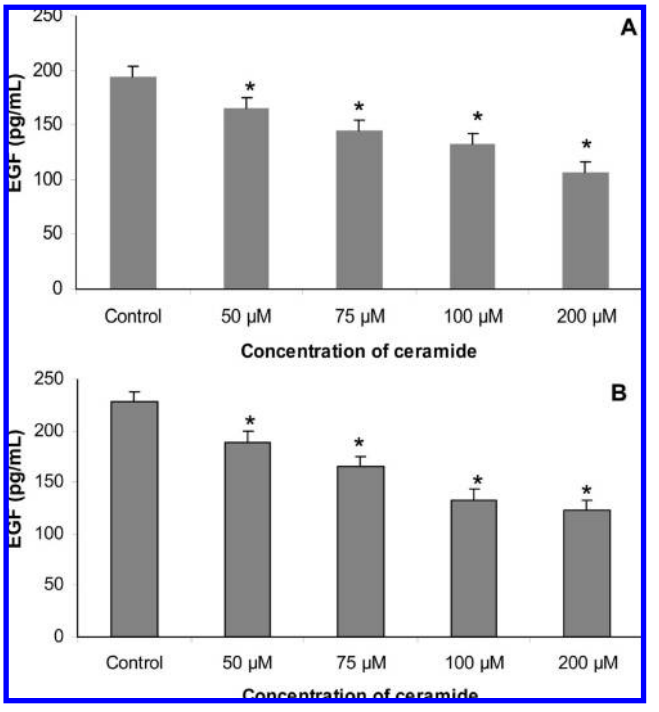

Figure 5. Effect of CMAEPn on secreted EGF in cell cultures. Cells were serum-starved overnight and exposed to 0−200 μM CMAEPn (for MCF-7, A) or 0−500 μM CMAEPn (for MDA-MB-435s, B) for 48 h before harvesting the conditioned medium. VEGF protein secreted in the medium was detected by ELISA assay. Data represent the mean values ± SEM of three replicates from at least three experiments. (*) $p < 0.05$ compared to the control cells.

CMAEPn dose-dependently inhibited tube formation within 6 h. At 50 μM ceramide, the capillary-like network of the EC matrix was completely disrupted, suggesting that CMAEPn strongly inhibited *in vitro* angiogenesis (**Figure 2**).

3.2. Inhibition of MCF-7 and MDA-MB-435s Viability. The effect of CMAEPn on normal breast fibroblast cells was evaluated. Cell viability was about 85% at the range of concentrations of ceramides used, suggesting that CMAEPn was not very cytotoxic to normal cells. CMAEPn dose-dependently inhibited MCF-7 and MDA-MB-435s cell viability and proliferation (**Figure 3**). MCF-7 cell viability was reduced to 76% with the treatment of 125 μM CMAEPn and 38% with the treatment of 250 μM CMAEPn (**Figure 3**A). At 500 μM, the number of viable cells was very low. CMAEPn at 125 μM reduced MDA-MB-435s cell viability to 85% of the control cells after 48 h of treatment. The proliferation of these cells was further reduced to 45% in the presence of 250 μM CMAEPn. Proliferation was reduced to 27% at 500 μM CMAEPn concentration (**Figure 3**B).

3.3. Inhibition of VEGF and EGF in MCF-7 and MDA-MB-435s Cancer Cells. CMAEPn dose-dependently inhibited the release of $VEGF_{165}$ in the condition medium (panels A and B of **Figure 4**). ELISA measurements indicated that control cells showed higher levels of VEGF and bFGF in the media than cells treated with CMAEPn. The VEGF levels in the controls of MCF-7 and MDA-MB-435s cells were 246 and 291 pg/mL, respectively. The levels of VEGF in 200 μM CMAEPn-treated MCF-7 and MDA-MB-435s were 115 and 145 pg/mL, respectively. CMAEPn also dose-dependently inhibited the release of EGF in the conditioned media of MCF-7 and MDA-MB-435s breast cancer cells (panels A and B of **Figure 5**). Controls MCF-7 and MDA-MB-435s contained 194 and 228 pg/mL EGF, respectively. The concentration of EGF in 200 μM CMAEPn-treated MCF-7 and MDA-MB-435s were 106 and 123 pg/mL, respectively (panels A and B of **Figure 5**).

3.4. Inhibition of Cell Migration and Invasion. MCF-7 cells are non-invasive, and we studied only the inhibition of MDA-MB-435s cell migration and invasion. CMAEPn dose-dependently inhibited the migration of MDA-MB-435s breast cancer cells in the presence

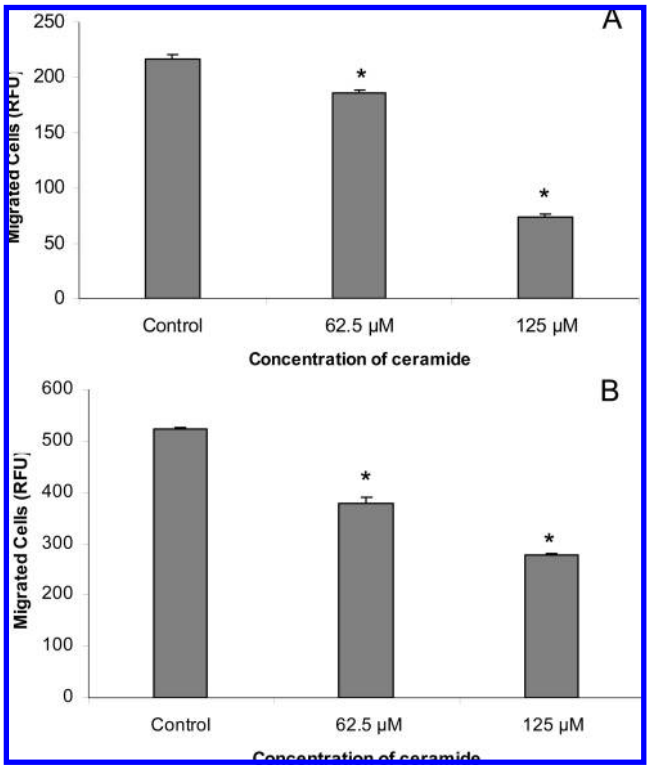

Figure 6. Effect of CMAEPn on MDA-MB-435s cell (A) migration and (B) invasion. MDA-MB-435s cells (1.0×10^6 cells for the migration assay and 2.0×10^6 cells for the invasion assay) were suspended in 0.1 mL in serum-free media, treated with DMSO (control) or CMAEPn (62.5 or 125 μM), and seeded in the upper chamber of the transwell. The wells of the lower chamber were loaded with 150 μL of media containing 10 ng/mL VEGF. After incubation for 6 h at 37 °C in a 5% CO_2 atmosphere, the cells that migrated through 8 μm pore size to the lower chamber were dislodged, lysed, and analyzed by fluorescence as described under Materials and Methods. Data presented are representative of three replicate experiments ± standard errors of relative fluorescence (RFU) of migrated cells. (*) $p < 0.05$ compared to the control cells.

of 10 ng/mL as a chemoattractant (**Figure 6**A). There was a significant inhibition of cell migration at the concentration of 125 μM ceramide after 48 h of incubation. CMAEPn also dose-dependently inhibited MDA-MB-435s invasion in the presence of VEGF as a chemoattractant, and the largest inhibition occurred at 125 μM (**Figure 6**B).

3.5. Inhibition of Caspase Activities and Induction of Autophagic Cell Death. Both MCF-7 and MDA-MB-435s breast cancer cells showed a significant dose-dependent decrease in caspase-9 activities (panels A and B of **Figure 7**). Caspase-3 activation is essential for caspase-9, caspase-7, and caspase-8 activation (*20*). MCF-7 cells lack pro-caspase-3 but contain detectable levels of pro-caspase-9 (*19*, *27*, *29*, *30*). In these cells, the lack of caspase-3 may contribute to the inability to detect caspase-9 activation or caspase-9 activation may not occur (*21*). Caspase activation is associated with cell death by apoptosis, whereas caspase inhibition is necessary to induce cell death by autophagy (*22*, *23*). Results in **Figure 7**A suggest that MCF-7 cell death was independent of caspase-3 activity. Caspase-9 depletion was also observed in MDA-MB-435s cells incubated with CMAEPn (**Figure 7**B). Cell death associated with delayed caspase-3 activation and caspase-9 depletion has been reported (*24*). Additional evidence of cell death by autophagy was provided by fluorescence microscopy following staining of control and CMAEPn-treated cells with the lysomotropic agent acridine orange incorporated in CMAEPn-treated MCF-7 and MDA-MB-435s cells (**Figure 7**). Staining of control untreated cells with acridine orange, a weak base, displayed predominantly green fluorescence with cytoplasmic and nuclear components, with very minimal red fluorescence. However, in acidic compartments, such as autophagolysosomes, the protonated form of acridine orange accumulated and displayed red fluorescence when observed by fluorescence microscopy (**Figure 8**). Both CMAEPn-treated MCF-7 and CMAEPn-treated MDA-MB-435s cells showed the presence of acridine orange in autophagic vacuoles compared to untreated control MCF-7 and MDA-MB-435s cells (**Figure 8**). Acridine orange has been used as a specific marker for autolysosomes (*17*, *18*), although recently it has been reported that acidotropic dyes, including acridine orange, LysoTracker Red, monodansyl cadaverine (MDC), and monodansylpentane (MDH), are not by themselves ideal markers because they primarily detect lysosomes (*25*). However, the acidotropic dyes can stain late autophagic vacuoles (*25*). Ceramide is considered to be an important factor in the regulation of autophagy (*26*). Autophagy is a caspase-independent process, and the blockage of caspase activity can cause cells to switch from apoptotic to autophagic cell death (*27*, *28*). However, it has been argued that the biochemical hallmarks of apoptosis (type-1 cell death) may be involved in the execution of autophagy (type-2 cell death), and beclin-1 has been identified as one critical molecule between apoptosis and autophagy (*29*).

3.6. Western Blot. To further confirm the results of the morphologic observations, we measured the levels of beclin-1 and PI3K in control and CMAEPn-treated MCF-7 and MDA-MB-453s cells. The levels of PI3K were downregulated in both cell lines (**Figure 9**A). Both MCF-7 and MDA-MB-435s controls showed the presence of PI3K and undetectable levels of PI3K in CMAEPn-treated cells (**Figure 9**A). Ceramide has been shown to interfere with the inhibitory class I PI3K signaling pathway to stimulate the expression of autophagy gene beclin-1 (*26*). Class I PI3K, Akt, and MTOR are components of the pathways involved in both apoptosis and autophagy. Western Blot results also showed that the protein levels of beclin-1 were upregulated in response to CMAEPn treatment in both MCF-7 and MDA-MB-435s cells (**Figure 9**B). We also observed that the increase in beclin-1 in both cells was completely blocked when an autophagy inhibitor 3-MA was used (not shown). Several studies have shown that the expression of beclin-1 was greatly reduced or non-existent in breast tumors and breast carcinoma cell lines, including MCF-7 and MDA-MB-435s; however, upregulation of beclin-1 at mRNA and protein levels in those cells was associated with the restoration of autophagic capacity (*26*). Beclin-1 expression was followed by altered expression of caspase-9 in cervical cancer HeLa cells (*30*).

3.7. Inhibition of IκBα Degradation and NFκB Activation. We examined whether CMAEPn regulates TNF-α-stimulated IκBα phosphorylation and degradation in MCF-7 and MDA-MB-435s cells. Our results show that CMAEPn dose-dependently inhibited TNF-α-stimulated IκBα phosphorylation and degradation (panels A and B of **Figure 10**) and NFκB p50/65 nuclear translocation (panels A and B of **Figure 11**). In the cytosol, NFκB is inactive via binding to IκB. NFκB becomes active through phosphorylation and degradation of IκB. Our results indicate that CMAEPn inhibits the phosphorylation and degradation of IκB in both cell lines. The results on nuclear translocation of p50/p65 also suggest that CMAEPn significantly suppressed the nuclear translocation of the heterodimers. NFκB suppresses autophagy, and inactivation of NFκB enhances autophagy possibly as a result of modulation of the beclin1/*bcl*-2 balance by NFκB because *bcl*-2 can interact with beclin-1 to control autophagy (*31*, *32*). However, it has been shown that

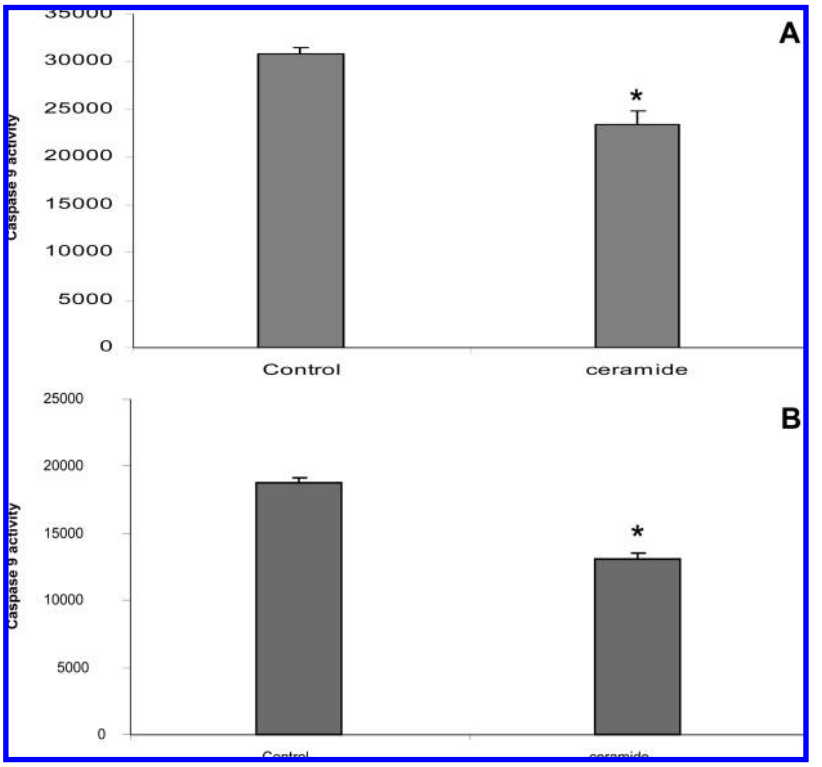

Figure 7. Determination of apoptosis by the caspase-9 assay. MCF-7 cells were seeded in 96-well plates and exposed to 0 (control) or 125 μM CMAEPn. MDA-MB-435s cells were seeded in 96-well plates and exposed to 0 (control) or 250 μM CMAEPn. Both cell lines were incubated for 48 h. At the end of the incubation period, the cells were treated with 100 μL of Caspase-Glo 9 reagent incubated for 1 h and the luminescence of the solution was measured using a Perkin-Elmer LS 50B luminometer. Each assay was conducted in triplicate and repeated at least 3 times. (A) Control and CMAEPn-exposed MCF-7 cells. (B) Control and CMAEPn-exposed MDA-MB-435s cells. (*) $p < 0.05$ compared to the control cells.

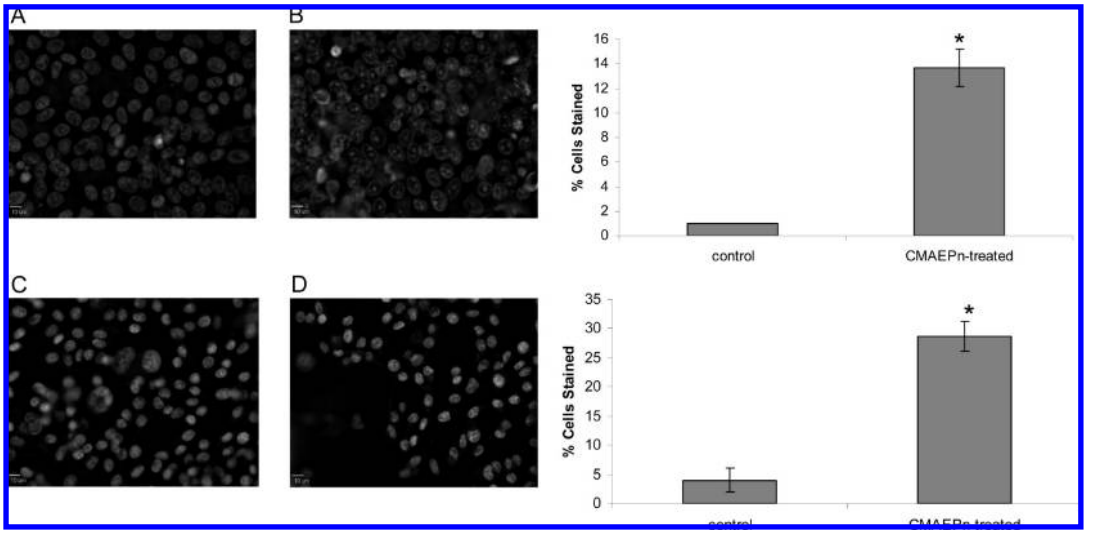

Figure 8. Detection of CMAEPn-induced autophagy by acridine orange staining. (A) MCF-7 were seeded in 6-well plates and exposed to 0 (control) or 125 μM CMAEPn for 48 h. MDA-MB-435s cells were seeded in 6-well plates and exposed to 0 (control) or 250 μM CMAEPn, respectively, for 48 h. The cells were incubated with 1 μg/mL acridine orange (Molecular Probes) in serum-free medium for 15 min. The acridine orange was removed, and fluorescent micrographs were obtained using an inverted fluorescence microscope, where green staining reflects the background and orange−red staining occurs in autophagic vacuoles. (B) Percentage of total cell population that stained for acridine orange was quantified. Data presented are representative of three replicate experiments ± standard errors (at a magnification of 40×). Autophagy was statistically significant in CMAEPn-exposed cells than control cells ($p < 0.05$).

inactivation of NFκB leads to cell death by autophagy or apoptosis (*33*).

3.8. CMAEPn Inhibition of *in Vivo* Angiogenesis. Results in **Figure 12** indicate that, after 7 days, bFGF induced angiogenesis in matrigel, whereas CMAEPn inhibited bFGF-induced angiogenesis. Results in **Figure 12**A show increased angiogenesis in bFGF-treated matrigel, while results in **Figure 12**B show a reduction of angiogenesis in the presence of CMAEPn. The optical density at 540 nm was taken to measure the hemoglobin concentration. The average hemoglobin concentration in control matrigels was 37.91 mg/mL, and the average hemoglobin concentration in CMAEPn-treated matrigels was 21.62 mg/mL, suggesting a 57% inhibition of blood levels with the ceramide treatment within 7 days.

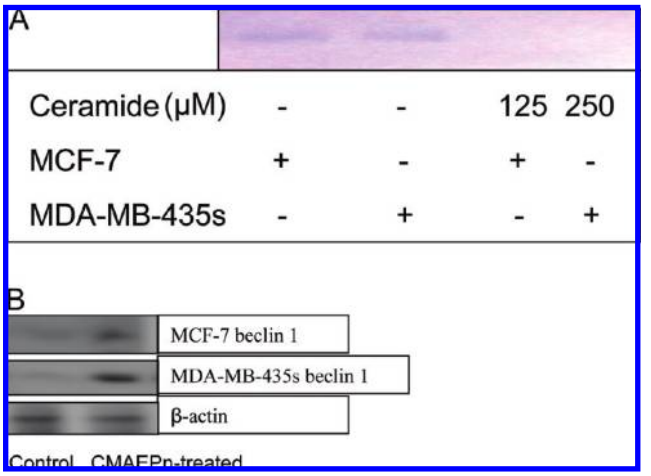

Figure 9. Effect of CMAEPn on PI3K and beclin-1 levels. MCF-7 and MDA-MB-435s cells were incubated with 0, 125, or 250 μM CMAEPn, respectively, for 48 h. Whole cell lysates were immunoprecipitated using anti-PI3K or anti-beclin-1 and analyzed by Western Blot with the indicated antibodies. (A) Inhibition of PI3K in MCF-7 and MDA-MB-435s by CMAEPn (B) Induction of beclin-1 in MCF-7 and MDA-MB-435s cells, respectively, by CMAEPn. Blots of anti-β actin are shown as a control for protein loading.

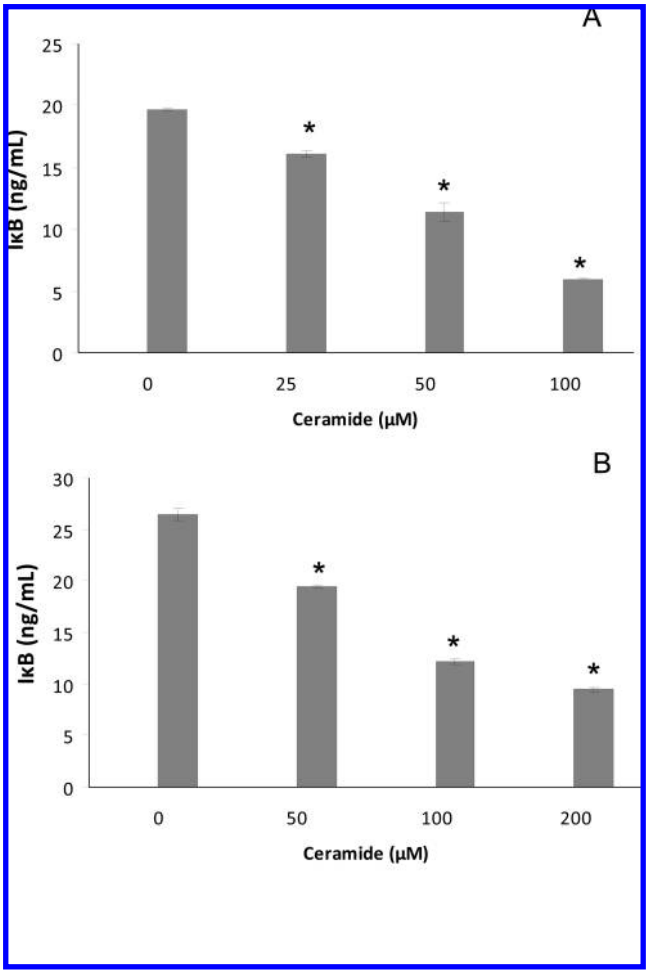

Figure 10. Effect of CMAEPn on IκB phosphorylation and degradation. MCF-7 and MDA-MB-435s cells were exposed to CMAEPn for 48 h in the presence of 10 ng/mL TNF-α. Cytoplasmic cell lysates were analyzed by ELISA. (A) Inhibition of IκB phosphorylation in MCF-7 cells. (B) Inhibition of IκB phosphorylation in MDA-MB-435s cells.

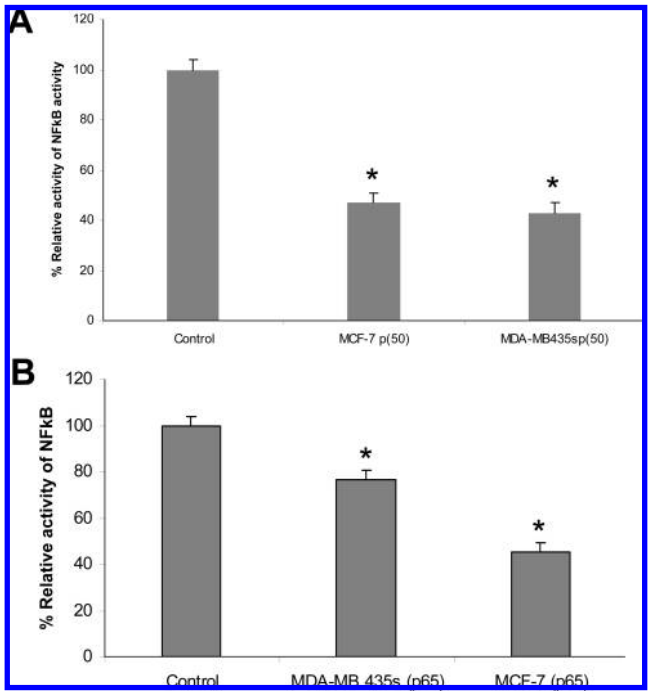

Figure 11. Effect of CMAEPn on NFκB DNA-binding activity. MCF-7 and MDA-MB-435s cells were exposed to CMAEPn for 48 h in the presence of 10 ng/mL TNF-α. Nuclear cell lysates for NFκB DNA-binding activity were analyzed by ELISA. (A) Inhibition of NFκB DNA-binding activity in nuclear extracts of MCF-7 cells by CMAEPn. (B) Inhibition of NFκB DNA-binding activity in nuclear extracts of MDA-MB-435s cells by CMAEPn.

4. DISCUSSION

Ceramides, the central molecules of sphingolipid metabolism, generally mediate antiproliferative responses, such as inhibition of cell growth and induction of apoptosis, and have emerged as a potential therapeutic strategy for inhibiting tumor progression. Evidence for the investigation of ceramides as potential tumor inhibitors has been based on several studies that showed that ceramides were significantly reduced in primary and metastatic tumor cells compared to normal cells in the same patients and treating tumor cells with exogenously or endogenously induced ceramides almost always led to cell apoptosis (*11*, *13*, *14*, *26*). However, recent studies have identified autophagy or type-2 programmed cell death (as opposed to type-1 cell death, also known as apoptosis), in which cells use different pathways for active self-destruction. Many cancer chemotherapeutics work by causing ceramide generation, and the latter is more toxic to tumor cells than normal cells. Growth factors promote cell growth and survival, and ceramides negatively regulate nutrient transport to cells. As result, ceramides have the ability to deprive cells of growth factors, block tumor cell initiation and metastasis, and induce autophagy (*14*). Because it is also well-established that cancer cells are more sensitive to ceramides than normal cells and chemotherapy works by causing ceramide generation, exogenous ceramides in the body may be toxic only to transformed cells, such as cancer cells. The present study was designed to evaluate the ability of CMAEPn from marine invertebrates to inhibit angiogenesis *in vitro* and *in vivo* and induce hormone-independent and -dependent breast cancer cell death. From the *in vitro* angiogenesis assays, it was found that 50 μM CMAEPn greatly inhibited the formation of tubules by endothelial cells in the presence of 10 ng/mL VEGF. CMAEPn also inhibited the viability of MCF-7 and MDA-MB-435s breast cancer cells. The inhibition of VEGF in MCF-7 and MDA-MB-435s cells by 49 and 46%, respectively, correlated with the ability of ceramides

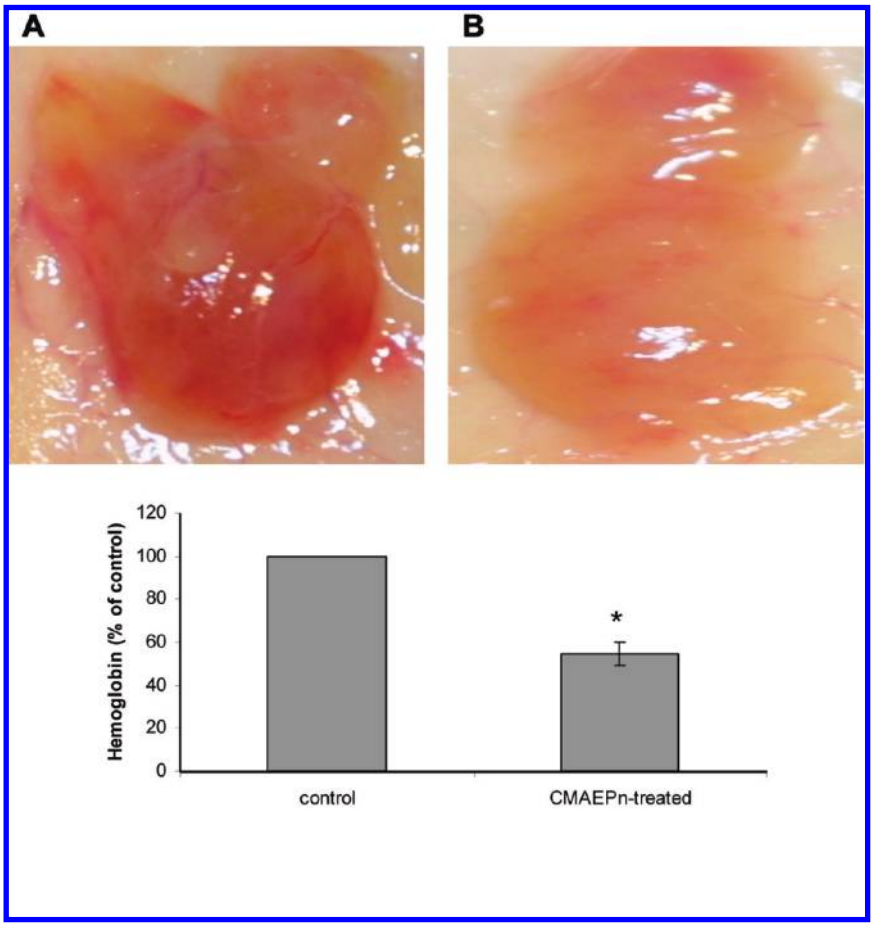

Figure 12. Effect of CMAEPn on matrigel plug assay. A total of 1 mL of matrigel mixed with 300 ng of bFGF was injected subcutaneously without CMAEPn on the left flank and with 30 mg/kg body wt of CMAEPn on the right flank of rats ($n = 5$). After 7 days, the matrigel plugs were carefully removed from underneath the skin, photographed, and analyzed for hemoglobin concentration using Drabkins reagent. (A) Matrigel containing 300 ng of bFGF. (B) Matrigel containing 300 ng of FGF and 30 mg/kg body weight of CMAEPn.

to deprive cancer cells of growth factors, causing those cells to die by autophagy. Similarly, CMAEPn through its ability as a ceramide to withdraw growth factors from cells reduced the levels of EGF in both MCF-7 and MDA-MB-435s breast cancer cells. Both MCF-7 and MDA-MB-435s breast cancer cells showed low caspase activity when treated with 125 and 250 μM ceramide, respectively. MCF-7 cells are known as caspase-3-deficient, and therefore, MCF-7 cell death should also be caspase-3-independent. Here, we also show that downregulation of growth factors, such as VEGF and EGF, in MCF-7 and MDA-MB-435s cells by CMAEPn stimulated autophagy by increasing the accumulation of positive autophagosomes in CMAEPn-treated cells. Results of Western Blot indicated that CMAEPn stimulated autophagy by upregulating the level of beclin-1 in both cell lines. Accumulation of beclin-1 correlates with cell death by autophagy. In MCF-7 and MDA-MB-435s cells, PI3K is activated. The results of Western Blot also indicate that CMAEPn inhibited the activity of PI3K in MCF-7 and MDA-MB-435s breast cancer cells, confirming the hypothesis put forth by Mukhamedova and Glushenkova (*8*). Recently, another group has associated solid tumor cell death by autophagy to inhibit PI3K activity in cancer cells (*34*). A synthetic phosphonolipid, 4-(hexadecyloxy)-3-(*S*)-methoxybutyl phosphonic acid (PoA), is a potent and specific inhibitor of PI 3-kinase (*35*). CMAEPn also inactivated NFκB, which promotes cell survival and proliferation. *In vivo* angiogenesis was assessed by matrigel plug assay. CMAEPn at 30 mg/kg body weight inhibited the formation of blood vessels *in vivo*. The results of the matrigel assay (**Figure 12**) show that treatment of EGF-stimulated matrigel with CMAEPn significantly inhibited EFG-stimulated angiogenesis and the ability of new blood vessels to invade the matrigel ($p < 0.05$) compared to untreated matrigel (control). These results may also be interpreted that ceramide inhibition of growth factor may have caused the inhibition of EGF-stimulated new blood vessel formation. Ceramide-treated matrigel plugs had lower values of hemoglobin than the controls, suggesting that less blood vessels were formed. Hemoglobin levels were 57% lower with the ceramide-treated cells. Overall, *in vitro* and *in vivo* assay results suggest that CMAEPn was effective against *in vitro* and *in vivo* angiogenesis and hormone-dependent MCF-7 and hormone-independent MDA-MB-435s breast cancer cell viability. The results of this study demonstrate that oyster ceramide inhibited angiogenesis *in vitro* and *in vivo*. Moreover, oyster ceramide inhibited the viability of hormone-dependent and -independent breast cancer cells by inactivating VEGF, EGF, and PI3K, which are some of the main signaling pathways associated with the progression of breast cancer. Many drugs including chemotherapy have been reported to trigger cell death by autophagy in cancer cells by increasing levels of endogenous ceramide (*26*, *36*). Ceramides do not necessarily induce cancer cell death by autophagy. Several studies have shown that the addition of exogenous ceramides to cancer cells trigger cell death by apoptosis or autophagy (*11*, *37*). Exogenous ceramides added to cancer cells accumulate in the mitochondria, leading to a decrease of the mitochondrial membrane potential, release of mitochondrial cytochrome *c*, activation of caspase-3 and caspase-9, and cell death (*11*, *13*).

Other studies in our laboratory have indicated that, *in vivo*, ceramide does not appear to induce apoptosis but does affect angiogenesis (*38*).

Marine bivalves and molluscans contain significant amounts of ceramides of different nature and size. Feeder species, such as oysters, molluscans, and menhaden fish (work in progress in our laboratory), concentrate ceramides of different nature depending upon the phytoplankton that these species filter. Work is in progress in our laboratory to identify the origin of the phytoplankton in which CMAEPn is concentrated. Oysters may contain ceramides other than CMAEPn and CMAEPn, and we are pursuing work to identify other ceramides and study their relationship to cancer cell activity *in vitro* and *in vivo*. The potential origin of CMAEPn and CMAEPn in the oyster is the result of an association with microalgae, because these sphingolipids are commonly found in phytoplankton.

ACKNOWLEDGMENT

We acknowledge Dr. Itonori, Chiba, Japan, for providing a sample of CAEPn for evaluation.

LITERATURE CITED

(1) Simon, G.; Rouser, G. Phospholipids of the sea anemone: Quantitative distribution; absence of carbon−phosphorus linkages in glycerol phospholipids; structural elucidation of ceramide aminoethylphosphonate. *Lipids* **1967**, *2*, 55–59.

(2) Matsubara, T. The structure and distribution of ceramide aminoethylphosphonate in the oyster (*Ostrea gigas*). *Biochim. Biophys. Acta* **1975**, *388*, 353–360.

(3) Matsubara, T.; Morita, M.; Hayashi, A. Determination of the presence of ceramide aminoethylphosphonate and ceramide *N*-methylaminoethylphosphonate in marine animals by fast atom bombardment mass spectrometry. *Biochim. Biophys. Acta* **1990**, *1042*, 280–286.

(4) Kariotoglou, D. M.; Mastronicolis, S. K. Sphingophospholipid molecular species from edible mollusks and a jellyfish. *Comp. Biochem. Physiol.* **2003**, *136*, 27–44.

(5) de Souza, L. M.; Iacomini, M.; Gorin, P. A.; Sari, R. S.; Haddad, M. A.; Sassaki, G. L. Glyco- and sphingophosphonolipids from the medusa *Phyllorhiza punctata*: NMR and ESI−MS/MS fingerprints. *Chem. Phys. Lipids* **2007**, *145*, 85–96.

(6) Zhukova, N. V. Lipid classes and fatty acid composition of the tropical nudibranch mollusks *Chromodoris* sp. and *Phyllidia coelestis*. *Lipids* **2007**, *42*, 1169–1175.

(7) Tamari, M.; Kandatsu, M. Occurrence of ceramide aminoethylphosphonate in edible shellfish, AGEMAKI, *Sinonovacula constricta*. *Agric. Biol. Chem.* **1986**, *50*, 1495–1501.

(8) Mukhamedova, K. S.; Glushenkova, A. I. Natural phosphonolipids. *Chem. Nat. Compd.* **2000**, *36*, 329–341.

(9) Karlsson, K. A.; Samuelsson, B. E. The structure of ceramide aminoethylphosphonate from the sea anemone, *Metridium senile*. *Biochim. Biophys. Acta* **1974**, *337*, 204–213.

(10) Matsubara, T.; Hayashi, A. Identification of molecular species of ceramide aminoethylphosphonate from oyster adductor by gas−liquid chromatography−mass spectrometry. *Biochim. Biophys. Acta* **1973**, *296*, 171–178.

(11) Radin, N. S. Killing tumors by ceramide-induced apoptosis: A critique of available drugs. *Biochem. J.* **2003**, *371*, 243–256.

(12) Shabbits, J. A.; Mayer, L. D. High ceramide content liposomes with in vivo antitumor activity. *Anticancer Res.* **2003**, *23*, 3663–3669.

(13) Struckhoff, A. P.; Bittman, R.; Burow, M. E.; Clejan, S.; Elliott, S.; Hammond, T.; Tang, Y.; Beckman, B. S. Novel ceramide analogs as potential chemotherapeutic agents in breast cancer. *J. Pharm. Exp. Ther.* **2004**, *309*, 523–532.

(14) Ogretmen, B.; Hannun, Y. A. Biologically active sphingolipids in cancer pathogenesis and treatment. *Nat. Rev. Cancer* **2004**, *4*, 604–616.

(15) Saddoughi, S. A.; Song, P.; Ogretmen, B. Roles of bioactive sphingolipids in cancer biology and therapeutics. *Subcell. Biochem.* **2008**, *49*, 413–440.

(16) Saito, H. Lipid and FA composition of the pearl oyster *Pinctada fucata martensii*: Influence of season and maturation. *Lipids* **2004**, *39*, 997–1005.

(17) Paglin, S.; Hollister, T.; Delohery, T.; Hackett, N.; McMahill, M.; Sphicas, E.; Domingo, D.; Yahalom, J. A novel response of cancer cells to radiation involves autophagy and formation of acidic vesicles. *Cancer Res.* **2001**, *61*, 439–444.

(18) Arthur, C. R.; Gupton, J. T.; Kellogg, G. E.; Yeudall, W. A.; Cabot, M. C.; Newsham, I. F.; Gewirtz, D. A. Autophagic cell death, polyploidy and senescence induced in breast tumor cells by the substituted pyrrole JG-03-14, a novel microtubule poison. *Biochem. Pharmacol.* **2007**, *74*, 981–991.

(19) Kottke, T. J.; Blajeski, A. L.; Meng, X. W.; Svingen, P. A.; Ruchaud, S.; Mesner, P. W.Jr.; Boerner, S. A.; Samejima, K.; Henriquez, N. V.; Chilcote, T. J.; Lord, J.; Salmon, M.; Earnshaw, W. C.; Kaufmann, S. H. Lack of correlation between caspase activation and caspase activity assays in paclitaxel-treated MCF-7 breast cancer cells. *J. Biol. Chem.* **2002**, *277*, 804–815.

(20) Prunet, C.; Lemaire-Ewing, S.; Ménétrier, F.; Néel, D.; Lizard, G. Activation of caspase-3-dependent and -independent pathways during 7-ketocholesterol- and 7β-hydroxycholesterol-induced cell death: A morphological and biochemical study. *J. Biochem. Mol. Toxicol.* **2005**, *19*, 311–326.

(21) Janicke, R. U.; Sprengart, M. L.; Wati, M. R.; Porter, A. G. Caspase-3 is required for DNA fragmentation and morphological changes associated with apoptosis. *J. Biol. Chem.* **1998**, *273*, 9357–9360.

(22) Yu, L.; Alva, A.; Su, H.; Dutt, P.; Freundt, E.; Welsh, S.; Baehrecke, E. H.; Leonardo, M. J. Regulation of an ATG7-beclin 1 program of autophagic cell death by caspase-8. *Science* **2004**, *304*, 1500–1502.

(23) Moretti, L.; Yang, E. S.; Kim, K. W.; Lu, B. Autophagy signaling in cancer and its potential as novel target to improve anticancer therapy. *Drug Resist. Updates* **2007**, *10*, 135–143.

(24) Georgakis, G. V.; Li, Y.; Rassidakis, G. Z.; Martinez-Valdez, H.; Medeiros, L. J.; Younes, A. Inhibition of heat shock protein 90 function by 17-allylamino-17-demethoxy-geldanamycin in Hodgkin's lymphoma cells down-regulates Akt kinase, dephosphorylates extracellular signal-regulated kinase, and induces cell cycle arrest and cell death. *Clin. Cancer Res.* **2006**, *12*, 584–590.

(25) Klionsky, D. J.; et al. Guidelines for the use and interpretation of assays for monitoring autophagy in higher eukaryotes. *Autophagy* **2008**, *4*, 151–175.

(26) Scaralatti, F.; Bauvy, C.; Ventrutti, A.; Sala, G.; Cluzeaud, F.; Vandewalle, A.; Ghindoni, R.; Codogno, P. Ceramide-mediated macroautophagy involves inhibition of protein kinase B and upregulation of beclin I. *J. Biol. Chem.* **2004**, *279*, 18384–18391.

(27) Lockshin, R. A.; Zakeri, Z. Apoptosis, autophagy, and more. *Int. J. Biochem. Cell Biol.* **2004**, *36*, 2405–2419.

(28) Vandenabeele, P.; Vanden Berghe, T.; Festjens, N. Caspase inhibitors promote alternative cell death pathways. *Sci. STKE* **2006**, *358*, No. e44.

(29) Liang, X. H.; Jackson, S.; Seaman, M.; Brown, K.; Kempkes, B.; Hibshoosh, H.; Levine, B. Induction of autophagy and inhibition of tumorigenesis by beclin 1. *Nature* **1999**, *402*, 672–676.

(30) Wang, Z. H.; Xu, L.; Duan, Z. L.; Zeng, L. Q.; Yan, N. H.; Peng, Z. L. Beclin 1-mediated macroautophagy involves regulation of caspase-9 expression in cervical cancer HeLa cells. *Gynecol. Oncol.* **2007**, *107*, 107–113.

(31) Pattingre, S.; Tassa, A.; Qu, X.; Garuti, R.; Liang, X. H.; Mizushima, N.; Packer, M.; Schneider, M. D.; Levine, B. Bcl-2 antiapoptotic proteins inhibit beclin 1-dependent autophagy. *Cell* **2005**, *122*, 927–939.

(32) Djavaheri-Mergny, M.; Amelotti, M.; Mathieu, J.; Besançon, F.; Bauvy, C.; Codogno, P. Regulation of autophagy by NFκB transcription factor and reactives oxygen species. *Autophagy* **2007**, *3*, 390–392.

(33) Simstein, R.; Burow, M.; Parker, A.; Weldon, C.; Beckman, B. Apoptosis, chemoresistance, and breast cancer: insights from

the MCF-7 cell model system. *Exp. Biol. Med.* **2003**, *228*, 995–1003.

(34) Coward, J.; Ambrosini, G.; Musi, E.; Truman, J. P.; Haimovitz-Friedman, A.; Allegood, J. C.; Wang, E.; Merrill, A. H.Jr.; Schwartz, G. K. Safingol (L-threo-sphinganine) induces autophagy in solid tumor cells through inhibition of PKC and the PI3-kinase pathway. *Autophagy* **2009**, *5*, 184–193.

(35) Lauener, R.; Shen, Y.; Duronio, V.; Salari, H. Selective inhibition of phosphatidylinositol 3-kinase by phosphatidic acid and related lipids. *Biochem. Biophys. Res. Commun.* **1995**, *215*, 8–14.

(36) Lavieu, G.; Scarlatti, F.; Sala, G.; Carpentier, S.; Levade, T.; Ghidoni, R.; Botti, J.; Codogno, P. Regulation of autophagy by sphingosine kinase 1 and its role in cell survival during nutrient starvation. *J. Biol. Chem.* **2006**, *281*, 8518–8527.

(37) Fillet, M.; Bentires-Alj, M.; Deregowski, V.; Greimers, R.; Gielen, J.; Piette, J.; Bours, V.; Merville, M. P. Mechanisms involved in exogenous C2- and C6-ceramide-induced cancer cell toxicity. *Biochem. Pharmacol.* **2003**, *65*, 1633–1642.

(38) Bansode, R. R. In vitro and in vivo anti-angiogenic activities of milk sphingolipids. Ph.D. Dissertation, Louisiana State Univerity, Baton Rouge, LA, Oct 2005.

Received December 9, 2008. Revised manuscript received March 23, 2009. Accepted April 24, 2009. This study was completed with a research grant from the Louisiana Agricultural Experiment Station and National Sea Grant Program through Louisiana Sea Grant.